A Photovoltaic Based Multilevel Inverter Fed Induction Motor Drive

M. Raja Nayak[a], M.Saritha[b], Syed Abdul Mujeer[c], B.Devulal[d], T.Santhosh Kumar[e]
[a,b,c,d,e]Assistant Professor, EEE department,
[a,c] Lakireddy Bali Reddy College of Engineering, Mylavaram. India.
[b]Matrusri Engineering College, Hyderabad, India.
[d]V N R Vignana Jyothi Institutre of Engineering and Technology, Hyderabad, India
[e] Lords Institute of Engineering and Technology, Hyderabad, India
[a]Email id: mrajanayak4260@gmail.com

Article History: Received: 11 January 2021; Revised: 12 February 2021; Accepted: 27 March 2021; Published online: 28 April 2021

Abstract: This paper proposes two new DC / AC multi-level hybrid bidirectional cells. PV MPPT method is used for the first cell. The second cell is called 5L – Parallel – BV (PBV) and has 5 voltage levels (5L). It is based on two parallel link groups of stacked HF cells, with two coupled inductors (CIs) and one simple cell. The use of two CIs is an interesting feature of the 5L – PBV cell. These CIs only operate on a half-cycle alternatively, with the CI inductor winding currents naturally set at 0. This paper is linked to the 3-phase 5L-PBV serial photovoltaic module. The advantage is that, with no output distortion of AC voltage due to unbalanced dc unit stress, the voltage of each DC in a multi-level inverter can be controlled. This theory allows PV system MPPT control to be easily carried out and the electricity produced overall is increased. The recent development of multiple-level inverter technology has been very important in the field of current control and high power. By using these inverters, we can adjust the induction motor's frequency levels without changing the input power. This article presents an experimental analysis and calculation of the bearing power for the 3-phase Induction motor linked to the 5L – PBV inverter circuit in three phases. The proposed switching cell requires a new three-stage, multi-level inverter. Finally, the induction motor is connected to the 3 phase multi-phase inverter output. Through the use of the photovoltaic cell, the speed and strength of the electromagnetic torque are controlled. The layout is an input source for the PV induction engine. The results are checked using the software MATLAB Simulink

Keywords: PV system, MMPT, 3-phase Induction motor, multilevel inverters, switching cells, parallel connection of switching cells, torque

1. Introduction

In recent years there has been an important increase in interest in multi-level power conversion. The advantages of multi-level topologies [1] are due primarily to this: Reduce the voltage converter turned on; Enhancing the output wavelengths quality; increase the apparent frequency of switching; Reduce the current ripple output. The basic definition for new multi-level converters development includes the three-level neutral – clamped (3L – NPC) topology [2], basic-topology cascade connections [3], Flying – Capacitor [4], and Coupled – Inductor (CI) principles [5]. A modern, unidirectional switching cell 3L – CI 3-phase inverter was presented with two-level (2L). New 5L inverters have been produced in [7] and [8] based on this principle. The key benefit of these topologies is that time is reduced. The high-frequency output harmonic currents have also been strengthened. The new single-phase five-level converter was proposed in [9] with the use of a CI principle and a DC voltage source (not separated by a DC voltage condenser). New multilevel Stacked – Flying – Capacitor (SFC) inverters were proposed in recent years[10] – [12], to increase the input voltage level and decrease the stored energy in FCs. Additional new multilevel topologies, involving integrated gate-commutated thyristors (IGCTs), gate-changed thyristors (GTOs), and insulated gate bipolar transistors (IGBTs), were offered using a hybrid approach in synergy. The multi-level topology in [13] blends the FC concept's versatility with the power of the Active-NPC (NPC) industrial converter. In[14] another hybrid approach was suggested that the versatility of the CI definition will be combined with the solidity of the industrial ANPC framework. It has mainly been designed to increase the output flow while reducing the current tension in power systems. Also, operation with the multilevel inverters shows key importance in high voltage power transmission systems [15].

In coloring, dust, and disparity in aging modules, the IV characteristics of the string modules cause variations, leading to several local maximum power points in the P-V string [2]. Complex MPP techniques are discussed for the monitoring of the global MPP [3]. The serial photovoltaic modules, as shown in Fig. 1, can be divided into different groups which become the dc units of the multi-level converter.

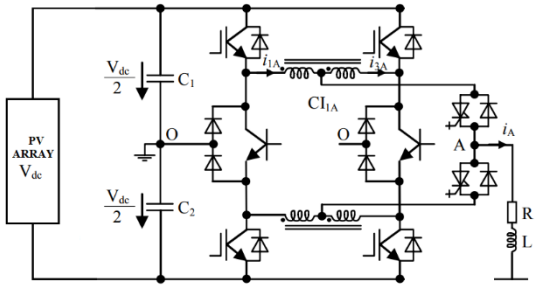

Fig.1, series-connected photovoltaic

Then you can individually change the voltage of these DC units so that you get independent MPPT control and minimize the partly shading effect. The above issues are detailed in this paper when the topology is a 5L-PBV inverter in three phases with 2 photovoltaic groups (Fig.1). The goodness of the proposed plan is also tested by simulation and experimentation.

The previous study shows PWM is a common voltage generator in the mode itself [1]. As the regular mode flows into the ground of the device, a rapid transition causes the voltage in the rotor shaft of the IM. This induced rotor voltage induces flow and flows from the rotor to earth through the tank and contributes to EDM motion at the inner course [1, 3, and 4]. The life of the bearing decreases thanks to the EDM.

It should be remembered that the sum of the three phase balanced voltages of sinusoidal is equal to zero at a three phase IM star point. Popular mode = C dv / dt, therefore. $V_{nq} = (V_{an}+V_{bn}+V_{cn})/3$ Where "C" is the system's overall power. The latest generation bearing mechanism is seen [2, 3]. The common-mode voltage at stage A is VAO with the inverter negative dc bus as a reference. The investigation of emissions bearing current and the point of star from IM to ground voltage is discussed below: Different methods were proposed for reducing the transient voltage from IM to ground at the star point and Shaotang Chen bearing current [4]. Introducing a passive filter system, David hypo [5] also suggested a new filter method for Yo-Chan Son & Seung-Ki Sul [6]. The application of the three-phase 5L – PBV inverter method for feeding a three phase inductive motor is discussed in this paper. This article presents the high-frequency phase that switches just half the output current, while the low-frequency phase switches the full induction motor output waveforms to the inverter with a 3-phased 5L – PBV inverter.

2. Literature Review

A. Three-level Unidirectional–Vienna (3L–UV) rectifier

A three-stage bidirectional PWM multi-stage corrective was implemented to reduce the harmonic components of the input current. An additional power device was required per step to generate three voltage levels. This 3L structure was translated into a boost unidirectional topology. The other unidirectional 3L PWM corrective variants were proposed in a Vienna rectifier. The famous 3L structure of the published topology is UV rectifier (Fig.2). Vienna (UV).

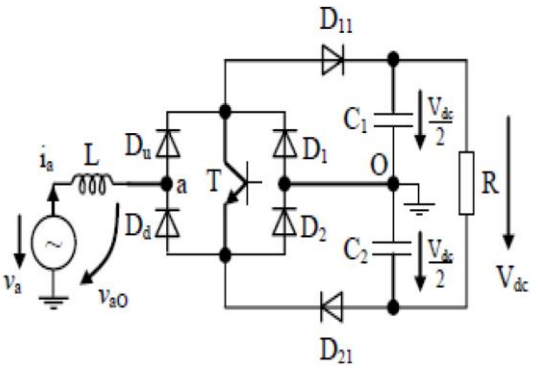

Fig.2. Three-level unidirectional–Vienna (3L–UV) rectifier

It only has one active (T) semi-controller and lower current rippling compared to the 2L PWM rectifier, with the 3L-UV rectifier. This 3L topology ensures that the conversion is unidirectional and can only function in corrective mode. It is impossible to operate in inverter mode and reactive power generation is severely limited.

B. 3L– Bidirectional–Vienna

A new three-tier (3L) hybrid DC / AC bidirectional switching cell [Fig.3] is introduced in this article. It is called 3L – Bidirectional – Vienna (3L – BV) and can be connected to a power source. 3L – BV topology is new and is based on two cascading steps operated at various switching frequencies (high and low). The high frequency (HF) stage is unique for piled switching cells using a shared three-pole bidirectional power unit, while a 2L base switching cell is the low frequency (LF) stage. The paper introduces two classic 3L concepts: 3L – NPC-Topology and 3L – unidirectional – Vienna (UV) correction, along with the proposed 3L – BV switching cell.

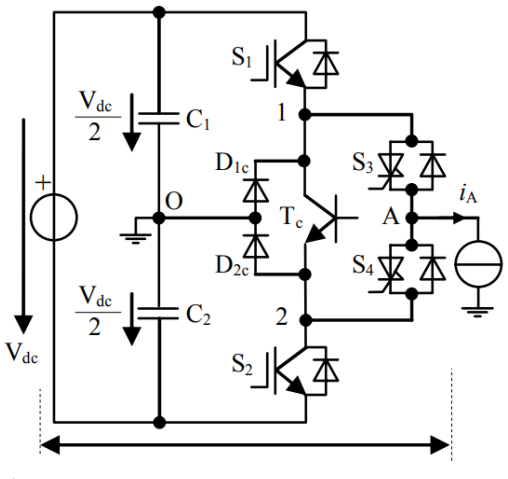

Fig. 3. Multilevel switching cells. (a) 3L–Bidirectional–Vienna (BV) topology.

C. Three-level NPC topology:

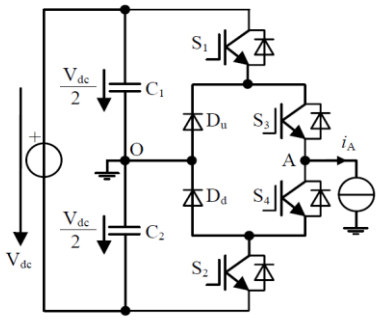

Fig.4 Three-level single–phase half–bridge NPC topology

The 3L-NPC converter is a two-way DC-AC topology that is commonly used in medium high-power applications. The field of research for low voltage applications (< 1000 V) has been broadened recently. 3L topologies derived from the NPC theory were recently suggested to boost performance. The 3L-NPC topology has only three moving states using a sinusoidal PWM (SPWM) technique. The S1 and S4 switches are operated for the whole cycle, each with S3 and S2 complementary. A loop is a reference voltage-time (v_r). The power supply regulation depends on the indication of the reference voltage. The power controller S1 and S4 is performed at switching frequency (f_{sw}) when the reference voltage of a sinusoid is positive, while S3 is activated and S2 disabled. The control of power devices is reversed when the sinusoidal reference voltage is negative. S2 and S3 are controlled at f_{sw}, and S1 is switched off and S4 activated. Consequently, just half of the cycle of voltage (Vdc/2) is switched from the four active voltage devices (S1 to S4).

D. BV Flipping Cell Of Three Stages

The proposed 3L topology, which comes from the principles of 3L – UV correction and 3L – NPC, is called Bidirectional – Vienna (3L – VVB) [Fig. 5]. For the first time in [11], a version of the 3 L-BV principles was implemented.

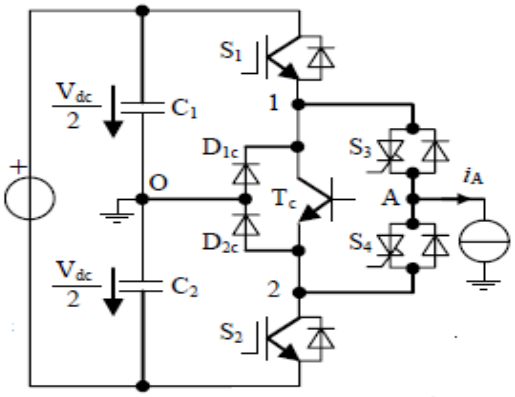

Fig.5 3L-BV Switching Cell

The only difference is that there is no anti-parallel diode needed for the active device (Tc). Topology is known as a hybrid because it involves semiconductive instruments that turn at various frequencies. The high-frequency (HF) high-swing is equivalent to three active power devices (S1, S2, T_c), whereas the low-frequency (LF) is equivalent to the reference frequency (f_r) of both active semiconductor devices (s3 and S4). The active instrument Tc is a bipolar transistor that needs no anti-parallel diode, to be highlighted. The S3 and S4 active power devices are presented as IGCT to emphasize low switching frequency operations.

E. NPC Topology Of Three Levels

The 3L NPC converter is a two-way DC-AC topology (Fig.6) primarily for applications with high power medium-voltage. The study area for low-voltage applications has been expanded by recent studies. 3L topologies derived from the NPC theory were recently suggested to increase efficiency [16].

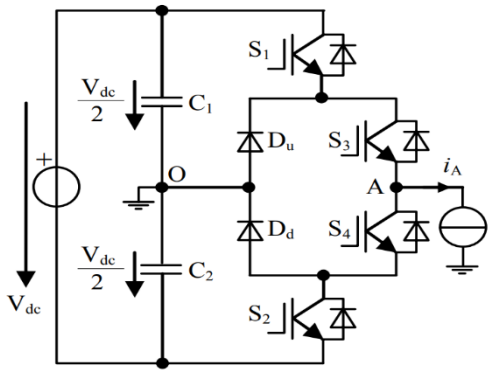

Fig. 6. Three-level single–phase half–bridge NPC topology.

The 3L-NPC topology has only three moving states using a sinusoidal PWM (SPWM) technique. The S1 and S4 switches are operated for the whole cycle, each with S3 and S2 complementary. A loop is a reference voltage-time (v_r). The power supply regulation depends on the indication of the reference voltage. The power controller S1 and S4 is performed at switching frequency (f_{sw}) when the reference voltage of a sinusoid is positive, while S3 is activated and S2 disabled. The control of power devices is reversed when the sinusoidal reference voltage is negative. S2 and S3 are controlled at f_{sw}, and S1 is switched off and S4 activated. As a result, just half of the cycle is shifted from four active power devices (S1 to S4) to half the voltage supply (Vdc/2). The average frequency of switching on a cycle (fav) is equal to f_{sw} (fav = fsw/2), while the apparent frequency of switching on the output voltage (fap) is equal to f_{sw} (SW).

F. Unidirectional Three-Level Viennese Corrector (3l-Uv)

A three-phase multilevel PWM rectifier was proposed in 1992[17] to minimize harmonic components of the input current. An additional power device was required per step to generate three voltage levels. This 3L structure was transformed in 1994[18] in a one-way boosting topology and called a Vienna rectification unit. Other 3L unidirectional PWM rectifier variants were subsequently proposed in 1996[19][20]. The most common 3L structure of Unidirectional – Vienna (UV) rectifier is the topology published in [20] (Fig.7).

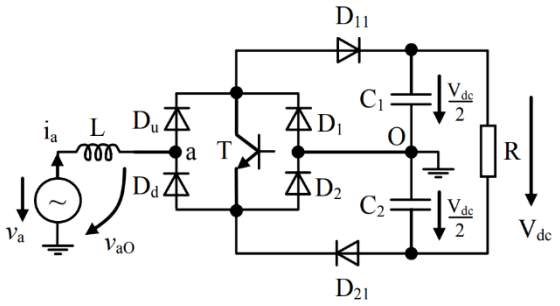

Fig. 7. Three-level uni-directional–Vienna (3L–UV) rectifier

Just one working semiconductor (T) unit has a working 3L-UV rectifier and lower ripples than the 2L-PWM rectifier. This 3L topology ensures that the conversion is unidirectional and can only function in corrective mode. It is impossible to operate in inverter mode and reactive power generation is severely limited. At the switching frequency (f_{sw}), the active power device (T) is regulated during the cycle and half of the output voltage is regulated (Vdc/2). Therefore the average frequency of switching (fav) in T and the apparent frequency of switching (f_{ap}) of the voltage of input (V_{ao}) equals f_{sw}.

G. BV Flipping Cell Of Three Stages

3L topology (3L – BV) [Fig.1 (a)] is called Bidirectional – Vienna (3L – BV), originating from 3L – UV corrective equipment and 3L-NPC definitions. For the first time in [21], a version of the 3L-BV principle was implemented. The only difference is that there is no anti-parallel diode needed for the active device (Tc). Topology is known as a hybrid because it involves semiconductive instruments that turn at various frequencies. The high-frequency (HF) high-swing is equivalent to three active power devices (S1, S2, Tc), whereas the low-frequency (LF) is equivalent to the reference frequency (fr) of both active semiconductor devices (s3 and S4). The active instrument Tc is a bipolar transistor that needs no anti-parallel diode, to be highlighted. The active power devices S3 and S4 are shown as IGCT to display a low frequency of operation. Tc and the two D1c and D2c diodes form a three-pole shift (Fig.8) with two bidirectional states (O-1 and O-2). Thus, two stacked HF switching cells consist of HF devices. S1 and SO1 are the first cell and only operate for the positive reference voltage. The other cell consists of S2 and SO2 and only deals with negative reference stress.

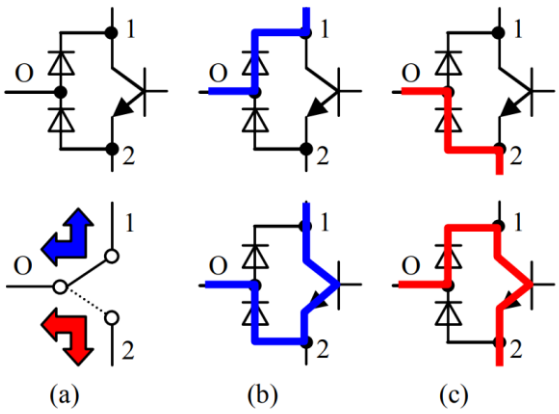

Fig. 8.Three–pole switch. (a) Symbol. (b) Switch SO1. (b) Switch SO2

The 3L – BV topology has four switching states, i.e. P, O1, O2, and N, using a sinusoidal PWM strategy (SPWM). The Tc switch is regulated at f_{sw} during the cycle, and S1 and S2 just half a cycle at f_{sw}. The 3L – BV switching cell proposed, therefore, has the following features:

(a) The S1 and S2 averages are equal to half (fav – S1 = fav – S2 = fsw/2); thus S1 and S2 both have losses and losses of switching;

(b) Tc's average switching frequency is f_{sw} (fav – Tc = f_{sw}); this T system switches at zero current when DC / AC is converted to the unit power factor;

(c) Active power units S3 and S4 only have a loss of conductivity; switching losses are negligible because they shift at the low frequency equal to the frequency of reference voltage (f_r);

d) f_{sw} (f_{ap} = f_{sw}) equals the apparent (effective) output torque switching frequency (fap). The 3L – BV switching cell for single-phase half bridge-PWM inverter with a load of an RL is validated in the paper author. A 3-phase 3L – BV converter can be obtained with three 3L – BV switching cells supplied with the same DC voltage. This arrangement can be used as a PWM or PWM inverter bi-direction. The proposed 3L-BV Switching Cell is not so desirable because of the greater number of active semiconductor devices than 3L – NPC. Its growth, however, is necessary to obtain new multilevel, high-performance static power conversion solutions.

H. 5L–Parallel–BV (PBV) topology

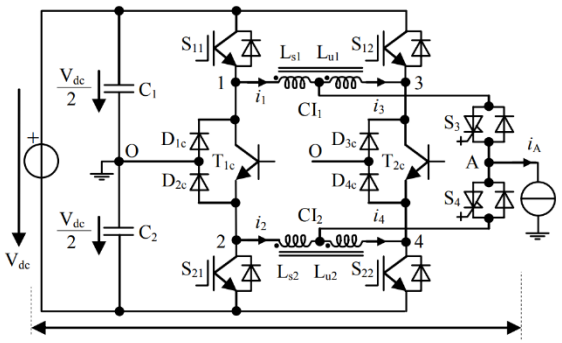

Fig. 9. Multilevel switching cells 5L–Parallel–BV (PBV) topology.

A new 5-level (5L) hybrid switching cell is also suggested with the 3L-BV principle [Fig.9]. 5L – Parallel-BV (PBV) converter is based on two groups of parallel, stacked HF-switching cells, which are linked via two coupling-inductors (CIs) and one simple 2L-cell (according to 3L – BV cell). The proposed 5L – PBV topology offers a convenient solution for low-voltage applications to increase the power supply while minimizing switching power in the HF stage. It can be used to build new multilevel bidirectional PWM converters with improved performance.

3. Single–Phase 5l–PBV Inverter

Fig. 10 for the first time introduces the proposed 5L – PBV switching cell. It consists of two cascading stags and two coupling inducers (CI1 and CI2) operated at different frequencies. The HF phase is unique to the parallel link between two groups of stacked switching cells in conjunction with 3L – BV, while the LF phase consists of a simple 2L switching cell.

The main DC voltage supply (Vdc) is divided into two secondary Vdc/2 link voltages, realized by two series of C1 and C2 connected condensers. All power equipment is priced at half the DC-link voltage (Vdc/2). To achieve bi-directional transmission of electricity, the new 5L switching cell can be connected between a voltage source and a current source. It can also be used for designing new topologies of PWM inverters/correctors.

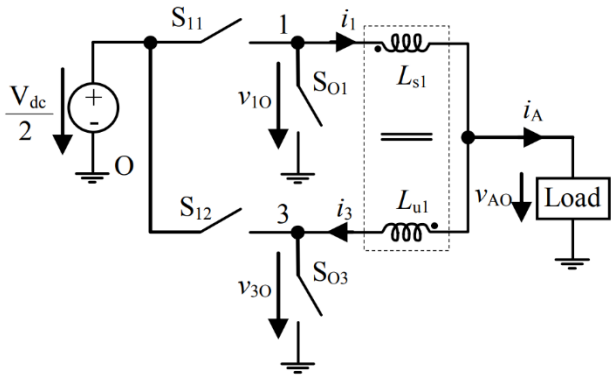

(a) Positive reference voltage

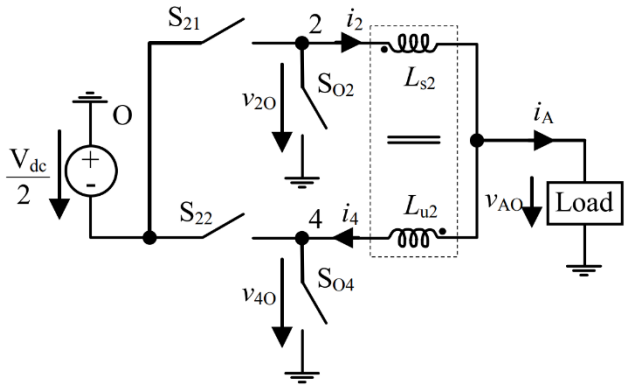

(b) Negative reference voltage

Fig. 10. Equivalent magnetic circuits of proposed 5L–PBV inverter. (a) the positive reference voltage (b) negative reference voltage

There are two identical circuits, depending on the reference voltage sign (Fig.10). In the single-phase half-bridge 5L – PBV inverter is regulated by the phase-shifted (PS) and the level-shifted (LS) techniques. Thus, a comparison of the sinusoidal reference voltage with four phase-level-shifted carriers (PLS) control of the active power devices is obtained. The originality of the proposed 5L – PBV inverter is that the difference of the currents in the inductor windings after each loop is automatically removed. The use of both CI for each arm allows the load current to be divided into high-frequency (HF) power devices in a balanced fashion, with the current being half the load current for each HF cell.

4. Photovoltaic (PV) System

A PV system transforms solar energy directly into electricity [22]. The PV cell is the fundamental unit for a PV system. Arrays may be divided into cells. The voltage and current on the PV unit can either be directly supplied by the power converter or connected to the power grid through small loads such as lighting systems and DC engines.

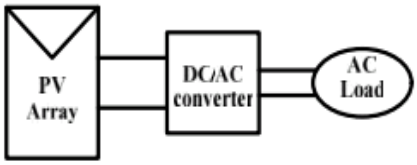

Fig.11. Block diagram representation of Photovoltaic system

This PV system comprises three main elements: PV module, system balance, and load. Photovoltaic system Charger, battery, and inverter are the main components of the system in these systems. The PV device block diagram is shown in Fig.11. A cell is essentially a semiconductive diode, the p-n junction of which is exposed to light. A variety of semiconductor types use different processes to manufacture photovoltaic cells. If the light incidence in the cell is short-circuited, charge carriers produce an electrical current.

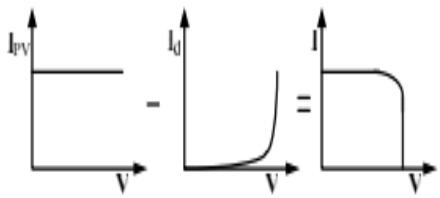

Fig.12. Characteristics I-V curve of the PV cell

Fig.12 displays the PV cell equivalent circuit. The PV cell is shown in parallel with the diode in the above figure by a current source. Rs and Rp are the series and parallel resistance. I-V characteristic of PV cell is shown in fig 8 Net-cell current I consisting of the current IPV produced by the light and the current ID diode. The I-V characteristics of the PV cell format are shown in figure 8.

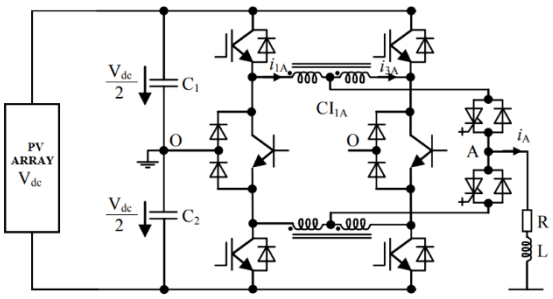

Fig.13 PV inverter with MPPT control

5. DC Voltage Control Units

With three levels inverter (Fig.13), Inp Term 0 only if bc connects to junction O, and then in one switching time we get an average Inp value (Inpav).

$$I_{\text{npav}} = \left(1 - \frac{|V'_{\max}|}{0.5V_{\text{dc}}}\right) \cdot I'_{\max} + \left(1 - \frac{|V'_{\min}|}{0.5V_{\text{dc}}}\right) \cdot I'_{\min} + \left(1 - \frac{|V'_{\text{mid}}|}{0.5V_{\text{dc}}}\right) \cdot I'_{\text{mid}}$$

I″, mid-I′, and min-I′ are phase currents that fit Vmax ″, Vmid′ and Vmin ″ phase legs. Equality. (7) it is important to simplify

$$I_{\text{npav}} = \frac{V^*_{\max} I'_{\max} + V^*_{\min} I'_{\min} + V^*_{\text{mid}} I'_{\text{mid}}}{-0.5V_{\text{dc}} \cdot (1+\varepsilon\delta)}$$

μ is the vector for a sign and μ= 1 for V_{min} \>0 in equation above; μ = −1 for Vmax < 0. In equation above. Eq.(6) can be extracted from $V_{offset2}$ field.

$$V_{offset2\min} < V_{offset2} < V_{offset2\max}$$

$$\begin{cases} V_{offset2\max} = \min\left\{ 0.5V_{dc} \cdot (1+\delta) - V_{\max}^*, -V_{\min}^* \right\} \\ V_{offset2\min} = \max\left\{ -0.5V_{dc} \cdot (1-\delta) - V_{\min}^*, -V_{\max}^* \right\} \end{cases}$$

Where max} {and min} {are to choose the larger one and to choose the smaller one of the two in}. After compensation the modulation waves are

$$\begin{cases} V'_{\max} = \dfrac{V^*_{\max} + V_{\text{offset2}}}{1+\delta} \\ V'_{\min} = \dfrac{V^*_{\min} + V_{\text{offset2}}}{1-\delta} \\ V'_{\text{mid}} = \dfrac{V^*_{\text{mid}} + V_{\text{offset2}}}{1+s\delta} \end{cases}$$

Where δ is the V * mid+Voffset2 symbol, I_{npav} can be entered as a replacement for Eq.(10) in Eq.(8).

$$I_{\text{npav}} = \frac{1}{-0.5V_{\text{dc}}} \left[\frac{V^*_{\max} \cdot I'_{\max}}{1+\delta} - \frac{V^*_{\min} \cdot I'_{\min}}{1-\delta} + \frac{s \cdot V^*_{\text{mid}} \cdot I'_{\text{mid}}}{1+s\delta} + V_{\text{offset2}} \cdot \left(\frac{I'_{\max}}{1+\delta} - \frac{I'_{\min}}{1-\delta} + \frac{s \cdot I'_{\text{mid}}}{1+s\delta} \right) \right]$$

If the referral voltage factor is μ *, the capacity of each dc unit is C, the frequency of change is f, and the unbalance factor can exceed μ * in a single switching cycle, it may be possible for us to achieve the following balance of the charge.

$$(I_{\text{npav}} - \Delta I_{\text{pv}})\frac{1}{f} = CV_{\text{dc}}(\delta - \delta^*)$$

Where Ipv is the difference of output current among the two classes of PV (Fig.3). Replace Eq.(11), we can obtain

$$V_{\text{offset2}} = \frac{a + sb}{c + sd}$$

Where a, b, c, and d are

$$\begin{cases} a = -0.5V_{\text{dc}}[V_{\text{dc}}Cf(\delta - \delta^*) + \Delta I_{pv}](1 - \delta^2) - V^*_{\text{min}}I'_{\text{mid}} + \\ \qquad \delta\left[V^*_{\text{min}}(I'_{\text{min}} - I'_{\text{max}}) + V^*_{\text{mid}}I'_{\text{mid}}\right] \\ b = -V^*_{\text{mid}}I'_{\text{mid}} \\ c = I'_{\text{max}} - I'_{\text{min}} \\ d = I'_{\text{mid}} \end{cases}$$

From Eq.(13) and Eq.(14), it can be inferred that the voltage of two dc units can be controlled by Voffset2 injection. The calculation of Voffset2 is not so straightforward since Eq.(9) and Tab.1 have been limited. As shown in Fig.4, the calculation flow can be synthesized.

If the two units' voltage is stable in Fig.3, we can deduce from Eq.(12), the MPPT Control Algorithm

$$I_{npav} = \Delta I_{pv} = I_{pv1} - I_{pv2}$$

The broader irradiance between PV1 and PV2 shows in Fig.2(a) the bigger the I_{pv} is. The above is not limited to Eq.(9), therefore, I_{npav} has a limit. As stated above. If I_{pv} does not reach the cap, the simple MPPT control algorithm is appropriate and the MPP can be controlled by each of the photovoltaic groups.

If the irradiance difference is significant and I_{pv} exceeds I_{npav}'s limits, the voltage of the higher-irradiance PV group must rise to allow the I_{pv} to fall to I_{npav} 's limits. The increase in voltage is to be determined by I_{npav} 's limit. For both power generation and systems reliability, there is a balance. Incremental action is used in this paper as the fundamental MPPT control algorithm [5]. In the following equation, the voltage relation is defined.

$$V_{ref(k)} = V_{ref(k-1)} + \gamma\frac{P_{(k)} - P_{(k-1)}}{V_{(k)} - V_{(k-1)}}$$

Whereas in K calculation duration, $V_{ref}(k)$, P(k), and V(k) are the references to the power of the PV group, real-time power, and real-time voltage. · DET is the voltage change incremental coefficient. Fig.5 displays the flow map of the stand-alone MPPT control algorithm.

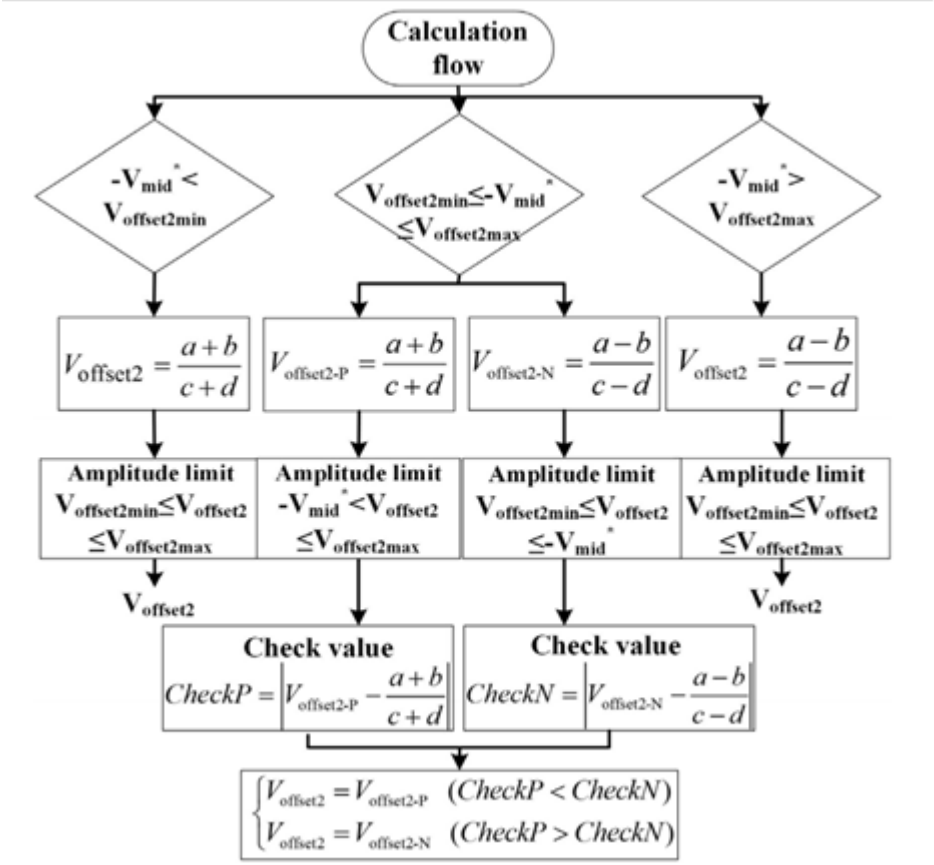

Fig. 14. The calculation flow of Voffset2

The low irradiance MPP of the PV group is first followed by the algorithm. If the voltage error falls within the Verror, this means that control margin remains in the control of the MPP; where a voltage error exceeds Verror, it means that the voltage error has reached a limited voltage level and the voltage relation falls increased in steps by step by Vstep to minimize the output current, it means that, if the voltage error exceeds the Verror The total output power of PV inverter can be maximized with this MPPT algorithm no matter how high the irradiance difference is

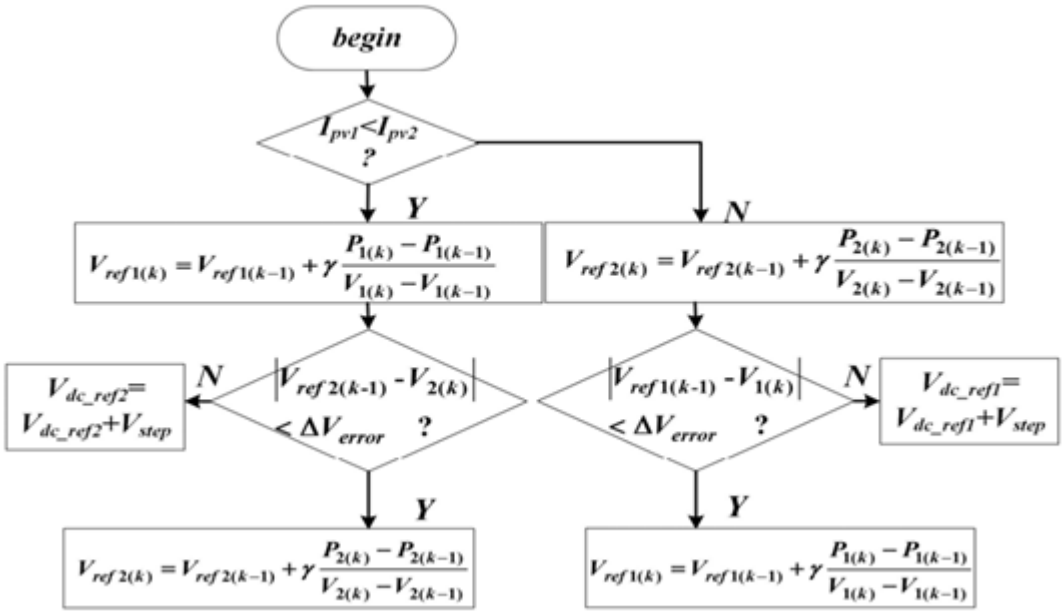

Fig. 15. The algorithm flowchart of independent MPPT control

Followers may be determined as following equations after Vref1 and Vref2 are obtained, the whole reference dc voltage Vdc * and the unbalance factor reference Vdc *.

$$\begin{cases} V_{dc}^{\ *} = V_{ref1} + V_{ref2} \\ \delta^* = \dfrac{V_{ref1} - V_{ref2}}{V_{ref1} + V_{ref2}} \end{cases}$$

6. Dynamics Of Induction Motor

In the stationary reference system shown in the figures below, a Squirrel cage Induction motor with Direct Axis and Quadrature Axis(d-q) theory requires fewer variables and easier analysis.

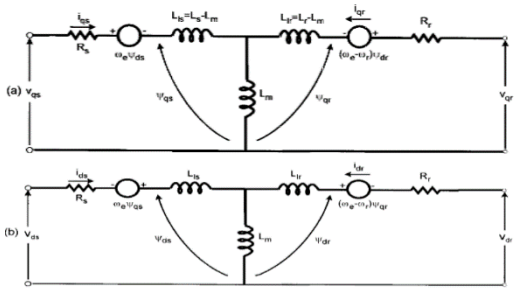

Fig.16. Stator and rotor axis in two axis reference frame (a) q-axis and (b) d-axis.

The transient electrical model can be used in matrix form in voltages and currents [5].

$$\begin{bmatrix} v_{qs} \\ v_{ds} \\ v_{qr} \\ v_{qr} \end{bmatrix} = \begin{bmatrix} R_s + SL_s & \omega_e L_s & SL_m & \omega_e L_m \\ -\omega_e L_s & R_s + SL_s & -\omega_e L_m & SL_m \\ SL_m & (\omega_e - \omega_r)L_m & R_r + SL_r & (\omega_e - \omega_r)L_r \\ -(\omega_e - \omega_r)L_m & SL_m & -(\omega_e - \omega_r)L_r & R_r + SL_r \end{bmatrix} \begin{bmatrix} i_{qs} \\ i_{ds} \\ i_{qr} \\ i_{dr} \end{bmatrix}$$

Normally speed is not processed as a constant. The torque can be connected to[12].

$$T_E = T_L + J\frac{dw_m}{dt} = T_L + \frac{2}{P}J\frac{dw_r}{dt}$$

7. Control Schemes Of Induction Motor

In essence, two general field-oriented control methods exist. They are the following:

(a) Direct Field Oriented Control,

(b) Indirect Field Oriented Control.

(a) Direct Field Oriented Control Method:

The name direct vector control [6] is provided by the generation of a vector signal from a feedback flux vector.

$$\cos\theta_e = \frac{\psi_{dr}^{s}}{\psi_s}$$

$$\psi_r = \sqrt{\psi_{dr}^{s^2} + \psi_{qr}^{s^2}}$$

The drive frequency is not regulated as in the scalar control in the vector control system directly. The machine is primarily automatic, where both the frequency and stage are indirectly regulated using the unit vector [3]. There is no fear of a problem of stability by crossing the point of action as a scalar control beyond the disintegration torque. The transitional response is as quick as DC since this approach does not affect the torque control of the stream. However, it is not possible to ideally vector control the converter and signal processing delays and the parameter variation effect in practice. Like a dc computer, speed control is possible without more control elements

in four quadrants [9]. If the torque is negative, the drive initially enters regenerative braking mode, which decreases speed. The unit vector phase series automatically reverses at zero speed and gives the reverse motor operation[11].

8. Existing Three Phase 5LPBv Inverter

A three-phase 5L-PBV inverter in this segment is proposed based on the 5L-PBV definition (Fig.9). The topology is regulated by CSVPWM, a technique that better addresses the emphasis of the vectors in each shift time. It is noted that this paper does not aim at optimizing the PWM strategy. The principle 3L – BV was used to create the Parallel – BV (5L – PBV) second hybrid five-level cell that switches to enhanced performance. It is also based on two cascaded phases, but the high-frequency stage shifts just half of the current, and the low-frequency phase switches over the whole current. It is also regulated at various frequencies. Numerical simulations for both single and three-phase inverter topologies have tested the mode of operation of the proposed concepts. The characteristics of these topologies are also presented and the findings obtained to support the theoretical research carried out

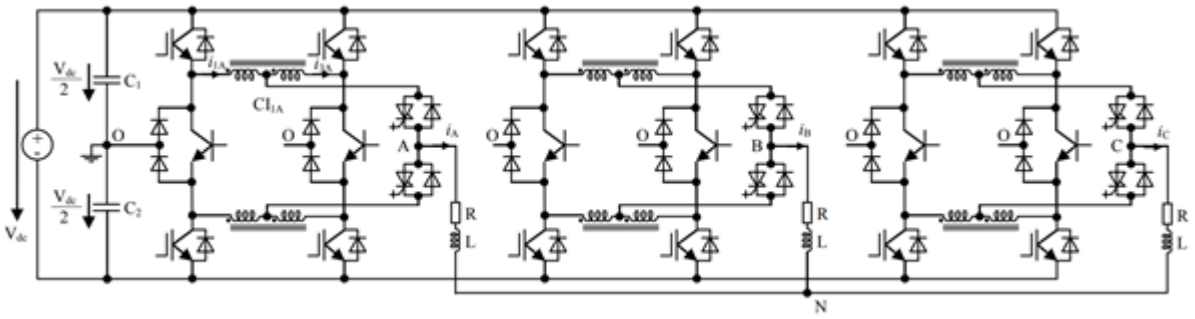

Fig. 17. Three-phase 5L–PBV inverter

9. Proposed Pv Three–Phase 5L–PBV Inverter With Induction Motor

Fig.10 for the first time introduces the proposed 5L – PBV switching cell. It consists of two cascading stags and two coupling inducers (CI1 and CI2) operated at different frequencies. The HF phase is unique to the parallel link between two groups of stacked switching cells in conjunction with 3L – BV, while the LF phase consists of a simple 2L switching cell.

The DC power output of the PV array should be converted via the inverter control into the three-phase high-quality AC power with the stability of current, provided the grid voltage is stable. Two serial linked capacitors (C1 and C2) divide into the PV output DC voltage (Vdc/2) into two secondary DC-link voltages (C1 and C2). All power devices are calculated at half the voltage of the DC-link(Vdc/2). To achieve bi-directional transmission of electricity, the new 5L switching cell can be connected between a voltage source and a current source. It is also possible to create new topologies for PWM inverters/rectifiers. Two equivalent circuits are obtained according to the reference voltage sign (Fig.6). The S3 system is allowed when $V_r>0$ is activated, while S4 is deactivated. The input voltage used for the parallel switching cells is positive and corresponds to half the DC – link voltage (Vdc/2). The center point (O) of the C1 and C2 series condensers is attached to the SO1 and SO3 switches, and the voltages v1O and v3O are positive on average. If VR<0, S4 is allowed while S3 is disabled. The S4 is allowed. The center point (O) of the series of condensers is connected with the SO2 and SO4 switches. The average values of v2O and v4O voltages are negative in this case.

The PS and LS methods are combined to monitor the 5L PBV single-phase half-bridge inverter. This is a simple phase-shifting technique. Thus a comparison of the sinusoidal reference voltage with four phase-level-shifted carrier (PLS) control of the active power devices is obtained. It has been observed that S11 and T1c power regulation, respectively S12 and T2c, are only controlled complementarily at half the cycle if the benchmark voltage is positive. The S11 and S12 controls are phase-shifted to 180 ° (vr>0) for this scenario. The S21, T1c, T2c, and S22 power supplies are similarly monitored for vr<0. Analysis of the ideal magnetic equivalent structures without energy storage (Fig.5) shows that the voltage of the magnetic structure is positive for reference voltage.

$$v_{10} - v_{A0} = v_{A0} - v_{30} \quad (1)$$

The output voltage is then defined

$$v_{A0} = (v_{10} + v_{30})/2 \quad (2)$$

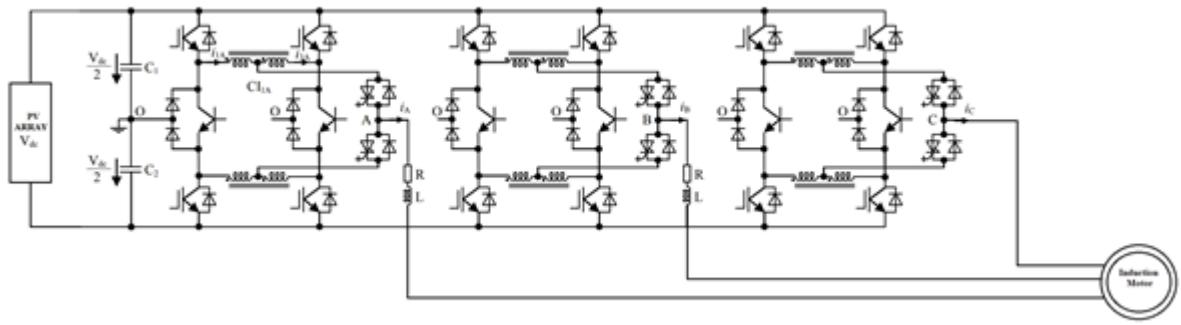

Fig.18. Proposed Three Phase 5L-PBV Inverter with PV array Induction Motor.

The originality of the proposed 5L – PBV inverter is that the difference of the currents in the inductor windings after each loop is automatically removed. The use of both CI for each arm allows the load current to be divided into high-frequency (HF) power devices in a balanced fashion, with the current being half the load current for each HF cell. The switched and drive currents are decreased for the HF switches:

$i_1 = -i_3 = i_A/2$

The increase in the output voltage levels to five (5L) in comparison to the 3L – BV structure is another aspect of this structure. In addition to this, two times the frequency of switching of the output voltage tends to be:

$f_{ap} = 2.f_{sw}$

These advantages contribute to the reduction, size, and expense of the output filter, in the loss of switching in HF power devices. The difference of currents by the inductors winding of CI1 (i1 and i3) gives the output currents for the positive voltage:

$i_A = i_1 – i_3$

A digital simulation of a single-phase half-bridge PWM inversion system with an RL load validates the 5L – PBV switching cell. Fig.8 shows some simulation findings. The output voltage has 5 levels [Fig.8(a)], the charging current is balanced in CI windings, and the inductor winding currents are normally set to null after each loop [Fig.8(b)]. The load current is divided into three levels.

A three-phase 5L-PBV inverter in this segment is proposed based on the 5L-PBV definition (Fig.9). The topology is regulated by CSVPWM, a technique that better addresses the emphasis of the vectors in each shift time.

It is noted that this paper does not aim at optimizing the PWM strategy. First, modulation at phase-level-shifted (PLS) can be expanded to include the typical offset mode in the reference voltages V_{rA}, V_{rB} and V_{rC} of three phases, as described in [14]. This offset comprises a third harmonic portion from

$$v'_{rk} = v_{rk} - \frac{\max(v_{rA}, v_{rB}, v_{rC}) + \min(v_{rA}, v_{rB}, v_{rC})}{2}$$

where k= A, B, C

The voltage references v_{rk} 'shall be transferred in a second step to a common carrier band [0, 1] by the following modulo function

$$v''_{rk} = \left(v'_{rk} + 1\right) \bmod (1)$$

Where the rest of the division (a / b) is supplied (a mod b). The further offset of the transformed v_{rk}'s indicators ensures that in each switching cycle the middle two space vectors of the switching series are oriented. Vrefk, including all offsets, is given the final voltage references

$$v_{refk} = v_{rk}^{'} + \frac{1}{2} - \frac{\max(v_{rA}^{''}, v_{rB}^{''}, v_{rC}^{''}) + \min(v_{rA}^{''}, v_{rB}^{''}, v_{rC}^{''})}{2}$$

The 5L – Parallel – Bidirectional – inverter Vienna has an interesting property to use with each arm of two CIs. The CIs of an arm therefore only operate on a half cycle and naturally the currents in inductor windings after each cycle are set to zéro. This implies that any difference between the currents in the inductor windings is constantly set to zero. By using the PWM inverter, we achieved better efficiency with the multi-level inverter and results were seen to be excursive. The three-level induction motor performance improvements. This work provides an extensive explanation of the theory of direct vector control and the current model of the motor. The drive system mathematical model was developed and results simulated.

10. Simulation Results

Here the simulation results are carried out in 3different cases

1) single–phase half–bridge 5L–PBV inverter

2) Three-phase half-bridge 5L–PBV inverter

3) Three-phase half-bridge 5L–PBV inverter with induction motor

Case-1 single–phase half–bridge 5L–PBV inverter

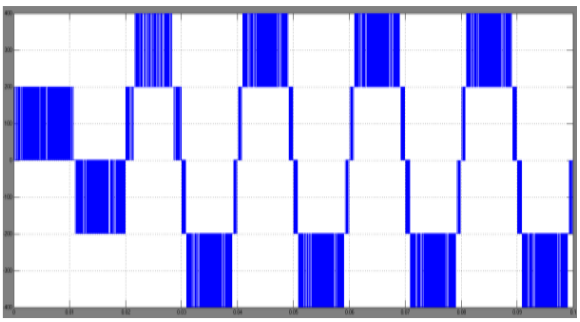

Fig.19 simulation output waveform of single–phase half–bridge 5L– PBV inverter

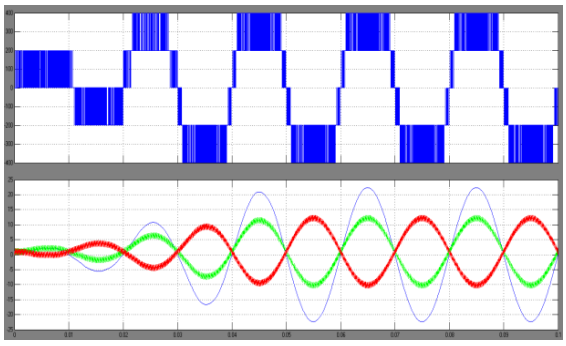

Fig20 Simulation results for the proposed single–phase half–bridge 5L–PBV inverter output voltage, output current

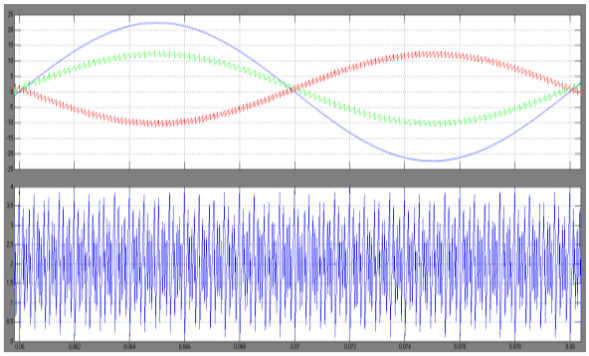

Fig.21. The output currents in inductor windings

Case-2 Three–Phase half-bridge 5L–PBV inverter

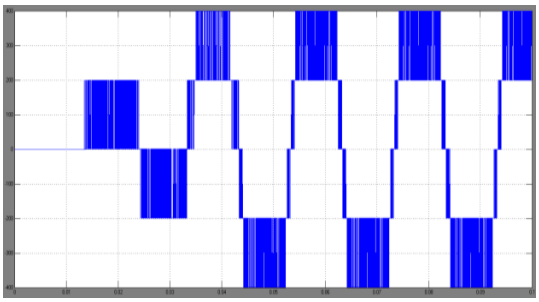

Fig.22 simulation output waveform of three-phase half-bridge 5L– PBV inverter

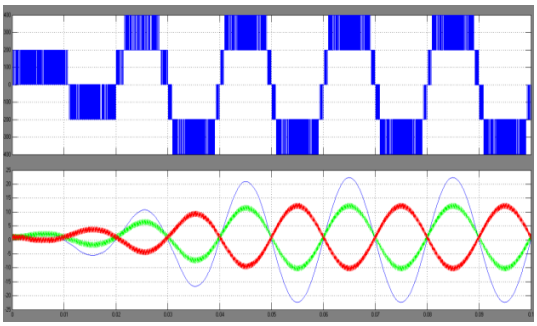

Fig.23 Simulation results for three-phase 5L–PBV inverter reference voltage for phase A, Line–to–line output voltage

Case-3 Three-phase half-bridge 5L–PBV inverter with induction motor

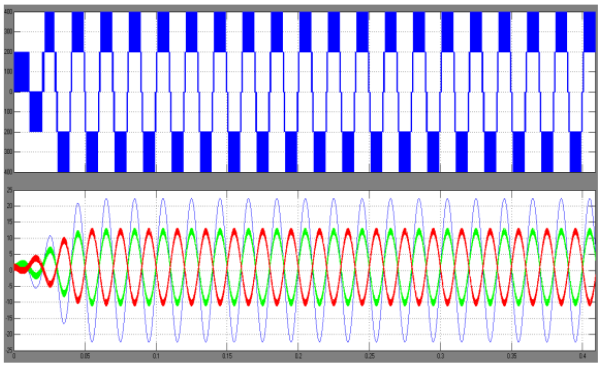

Fig.24. The three-phase inverter output voltage, output current

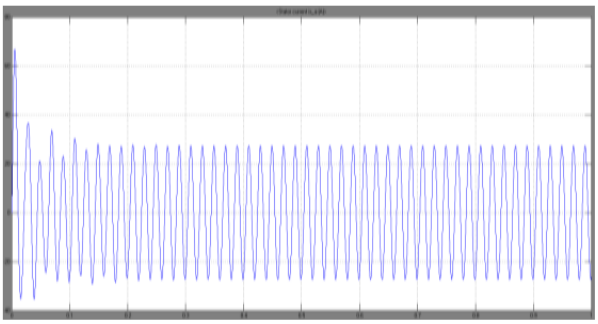

Fig.25 Armature current of induction motor

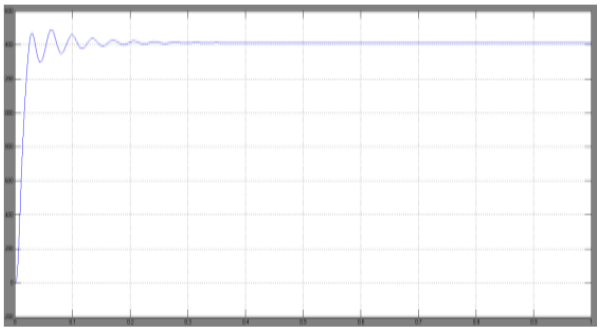

Fig.26 Speed of an induction motor

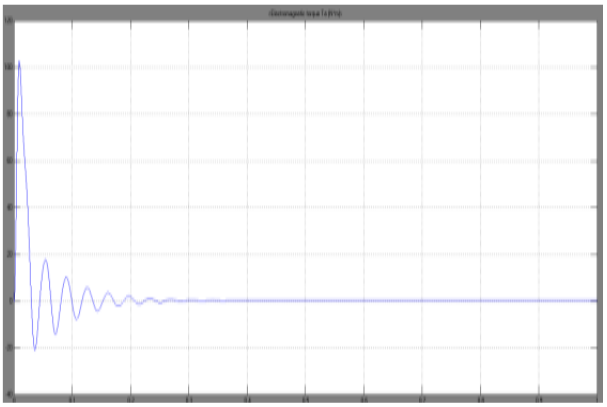

Fig.27. Electromagnetic torque of an induction motor.

11. Conclusion

A separate MPPT control device by the multi-level inverter is addressed in this paper to alleviate the inappropriate problem of connected PV modules with partial shading conditions. A detailed review of the control technique for three stages 5L – PBV is carried out such as noncorresponding compensation, independent stress control, and the MPPT algorithm. In this paper, the three-phase engine improvement output was presented using a multi-level inverter. With the multi-level method, the overall output current wave rate can be decreased by decreasing the output voltage value in stages, or by increasing the apparent output frequency of switching. Two new hybrid two-way DC-AC hybrid switching cells were presented in this work. You may link a voltage source to a power source. The First Solution is based on two different-from 3L – Bidirectional – Vienna (3L – BV) phases operated at various frequencies. The high-frequency stage requires two stacked switching cells with a 3-pole typical active power unit. In 5L – PBV, coupling inductors constitute an impediment to medium voltage applications with a low switching frequency. The proposed 5L topology is, therefore, an attractive solution for low-voltage applications, primarily for raising the output current, while reducing the current switched by the high-frequency power devices. Further, in terms of the voltage of the current probe output on the SVM system, there is no appreciable high-frequency change at the star point of IM to PV voltage and in the bearing current.

Acknowledgement

The authors are wish to thank the Management and Principal of Lakireddy Bali Reddy College of Engineering for their encouragement and permitting to publish this paper. Also, the Principals of MEC, VNRVJIT, LIET Hydearabad and GIET Rajamandry for their support to publish this paper.

References

1. T. S. Kumar, M. R. Nayak, R. V. Krishna and K. P. Rao, "Enhanced Performance of Solar PV Array-Based Machine Drives Using Zeta Converter," 2020 IEEE International Conference on Advances and Developments in Electrical and Electronics Engineering (ICADEE), Coimbatore, India, 2020, pp. 1-5, doi: 10.1109/ICADEE51157.2020.9368937.
    A. Bidram, A. Davoudi and R. S. Balog, "Control and Circuit Techniques to Mitigate Partial Shading Effects in Photovoltaic Arrays," Photovoltaics, IEEE Journal of, vol. 2, pp. 532-546, 2012-01-01 2012.

2. Patel and V. Agarwal, "Maximum Power Point Tracking Scheme for PV Systems Operating Under Partially Shaded Conditions," Industrial Electronics, IEEE Transactions on, vol. 55, pp. 1689-1698, 2008-01-01 2008.
3. Xie Luyao, Jin Xinmin, Wu Xuezhi, et al. Neutral point voltage feedback control based on zero sequence injection for three-level NPC converter[J]. Transactions of CES, 2012,24(12):101-111.
4. Yang Yongheng, Zhou Keliang. Photovoltaic cell modelling and MPPT control strategies[J]. Transaction of CES, 2011,39(4):229-234(in Chinese).
5. Mao Meiqin, Yu Shijie, Sujianhui. Versatile matlab simulation model for photovoltaic array with MPPT function[J]. Journal of System Simulation.2005,17(5):1248-1251 (in Chinese).
6. Bum-Seok Suh, and Dong-Seok Hyun, "A New -Level High Voltage Inversion System" IEEE Transactions on Industrial Electronics, Vol. 44, no. 1, February.
7. Jih Shenglai, Fang zhen Peng, "Multilevel converters-A new breed of Power converters"IEEE transactions on Industry applications.Vol.32, No3. May-June 1996.
8. Haoran Zhang, Annette Von Jouanne, Shaoan Dai, Alank. Wallace, Feiwang. "Multilevel inverter modulation schemes to eliminate common-mode voltages" IEEE transactions on Industry applications, Vol. 36, No.6. Nov-Dec. 2000.
9. Akira Nabae, Isao takahashi, Hirofumi Akagi" A new neutral point clamped PWM inverter". IEEE transactions on Industry applications, Vol.1a-17 No.5 Sep-Oct 1981.
10. Aneesh Mohamed A.S, Anish Gopinath & M.R. Baiju" A simple space vector PWM generation scheme for any general n-level inverter." IEEE transactions on Industrial Electronics, Vol. 56, No.5, May2009.
11. M. Saeedifard, P.M. Barbosa, and P.K. Steimer, "Operation and Control of a Hybrid Seven-Level Converter," IEEE Trans. Power Electon., vol.27, no.2, pp.652–660, Feb. 2012.
12. P. Barbosa, P. Steimer, J. Steinke, L. Meysenc, M. Winkelnkemper, and N. Celanovic, "Active neutral-point-clamped multilevel converters," in Proc. Power Electron. Spec. Conf., Recife, Brazil, pp.2296–2301, June 2005.
13. D. Floricau, E. Floricau, and G. Gateau, "New Multilevel Converters With Coupled Inductors: Properties and Control," IEEE Trans. on Ind. Electronics, vol.58, No.12, pp.5344–5351, Dec.2011.
14. M. R. Nayak and S. A. Mujeer, "New Computational Method for Study of Ionic Current Environment of HVDC Transmission Lines," 2020 IEEE International Conference on Advances and Developments in Electrical and Electronics Engineering (ICADEE), Coimbatore, India, 2020, pp. 1-5, doi: 10.1109/ICADEE51157.2020.9368934.
15. Y. Wang, and F. Wang, "Novel Three-Phase Three-Level-Stacked Neutral Point Clamped Grid-Tied Solar Inverter With a Split Phase Controller," IEEE Trans. Power Electon., vol.28, no.6, pp.2856–2866, June 2013.
16. T. Takeshita and N. Matsui, "PWM control and input characteristics of three-phase multi-level AC/DC converter," in Proc. Power Electron. Spec. Conf., pp.175–180, 1992.
17. J.W. Kolar and F.C. Zach, "A Novel Three-phase Utility Interface Minimizing Line Current Harmonics of High-Power Telecommunications Rectifier Modules", Record of the 16th IEEE International Telecommunications Energy Conference, Vancouver, Canada, Oct. 30–Nov. 3, pp.367–374, 1994.
18. H. Midavaine, P.L. Moigne, and P. Bartholomeus, "Multilevel three phase rectifier with sinusoidal input currents," in Proc. IEEE PESC'96, pp.1595–1599, 1996.
19. J.W. Kolar, H. Ertl, and F.C. Zach, "Design and experimental investigation of a three-phase high power density high efficiency unity power factor PWM (VIENNA) rectifier employing a novel integrated power semiconductor module," 11th IEEE Applied Power Electronics Conf., San Jose, CA, Mar. 3–7, vol.2, pp.514–523, 1996.
20. B. Cougo, G. Gateau, T. Meynard, M. Bobrowska-Rafal, and M. Cousineau, "PD Modulation Scheme for Three-Phase Parallel Multilevel Inverters," IEEE Trans. Ind. Electron., vol.59, no.2, pp.690– 700, 2012.
21. Kishor kumar Sadasivuni, Hitesh Pancha, Anuradha Awasthi, Mohammad Israr, F.A. Essa, S. Shanmugan, M. Suresh, V. Priya, Khechekhouche, " Ground Water Treatment using Solar Radiation-Vaporization & Condensation-Techniques by Solar Desalination system" International Journal of AmbientEnergy https://doi.org/10.1080/01430750.2020.1772872